Atmospheric Environment 94 (2014) 341–352

Contents lists available at ScienceDirect

Atmospheric Environment

journal homepage: www.elsevier.com/locate/atmosenv

Spatial variability of particle number concentrations and NO_x in the Karlsruhe (Germany) area obtained with the mobile laboratory 'AERO-TRAM'

Rowell Hagemann*, Ulrich Corsmeier, Christoph Kottmeier, Rayk Rinke [1], Andreas Wieser, Bernhard Vogel

Institute for Meteorology and Climate Research, Karlsruhe Institute of Technology, Postfach 3640, D-76021 Karlsruhe, Germany

HIGHLIGHTS

- We developed a mobile measurement system mounted on the roof of a tramcar.
- We perform long-term measurements during public transportation services.
- We examine spatial distributions of particle numbers and nitrogen oxides.
- Faster decline with significantly steeper gradient of NO_x outside the city area.
- Second increase of particle numbers without enhanced NO_x levels in the rural area.

ARTICLE INFO

Article history:
Received 5 July 2013
Received in revised form
14 May 2014
Accepted 16 May 2014
Available online 17 May 2014

Keywords:
Mobile measurements
Particle number concentration
Tramway
Urban pollution

ABSTRACT

For the first time in Germany, we obtained high-resolution spatial distributions of particle numbers and nitrogen oxides in an urban agglomeration using a tram system. In comparison to particle numbers the NO_x concentration decreased much faster with a significantly steeper gradient when going from the inner city to the surrounding area. In case of NO_x the decrease was 70% while for particle number concentration it was only 50%. We found an area in the rural surrounding with a second increase of particle numbers without simultaneous enhanced NO_x levels. The source of the high particle numbers could be ascribed to industry emissions about 5–10 km away. The mean spatial distribution of particle number concentration depended on wind direction, wind velocity and boundary layer stability. The dependency was particularly strong in the rural area affected by industrial emissions, where individual wind directions led to concentration differences of up to 25%. The particulate concentration was 40% higher during low wind velocities (1–5 m s^{-1}) than during high wind velocities (>5 m s^{-1}). We observed similar findings for the impact of boundary layer stability on particle numbers concentration. Particle pollution was 40% higher for stable stratification compared to neutral or unstable cases.

1. Introduction

In addition to influencing atmospheric radiation, cloud formation, and precipitation, aerosol particles affect human respiratory health. Epidemiological studies of Brunekreef and Holgate (2002), Katsouyanni (2003), Künzli et al. (2000), Pope et al. (2002) showed that there is a correlation between the aerosol mass concentration and mortality. All of these studies are mass based, which means the total particle mass of particles with diameters less than 2.5 μm (PM2.5) or less than 10 μm (PM10) was used. Based on these and other studies different directive proposals e. g. EC (2008) and WHO (2006) evolved that define the current threshold values.

Apart from the mass there are other physical and chemical parameters like size distribution, number concentration (PNC) and chemical composition to characterize the atmospheric aerosol and which are as well as relevant for human health (Pöschl, 2005). A critical point is the varying penetration depth in the respiratory tract depending on the particle diameter. Fine particles with diameters below 1 μm, which contribute only a minor amount of the

* Corresponding author.
E-mail addresses: rowell.hagemann@kit.edu (R. Hagemann), ulrich.corsmeier@kit.edu (U. Corsmeier), christoph.kottmeier@kit.edu (C. Kottmeier), u360424@stuttgart.de (R. Rinke), andreas.wieser@kit.edu (A. Wieser), bernhard.vogel@kit.edu (B. Vogel).
[1] Present address: Office for Environmental Protection of the city of Stuttgart, Section of Urban Climatology, Gaisburgstraße 4, D-70182 Stuttgart, Germany.

http://dx.doi.org/10.1016/j.atmosenv.2014.05.051

total particulate mass, are under suspicion in being more important for health than larger particles (e. g. Liu et al., 2013; Kampa and Castanas, 2008). Small particles, particularly with diameters below 0.1 μm, are the main contributor of particle number concentrations. Studies, concerning PNC, show connections between health and this aerosol parameter (e.g. Penttinen et al., 2001).

Besides road traffic and other emissions, meteorological conditions are an important factor for the spatial and temporal variability of aerosol particles and gaseous compounds. The spatial patterns can be modified by both local wind conditions (Rosenbohm et al., 2005; Väkevä et al., 2000) but also by the synoptic conditions (e.g. Gomišček et al., 2004; Johansson et al., 2007; Viana et al., 2003; van der Zee et al., 1998). Furthermore, there are other parameters that determine air quality, like precipitation or mixing layer height (e.g. Johansson et al., 2007; Väkevä et al., 2000; Viana et al., 2003; van der Zee et al., 1998).

The quantification of the impact of atmospheric processes on the spatial distribution of aerosols presents a challenge in urban areas. There, frequent changes of land-use influence meteorological processes at small scales which affect the conditions of local air dispersion. Both meteorological parameters and spatial aerosol distribution therefore show a high temporal variability in urban areas. Thus it is difficult to identify clear relations between meteorological conditions and concentrations. Evaluations of long-term measurements allow a quantification of meteorological influences like temperature, humidity, radiation, wind or mixing layer height, (Bukowiecki et al., 2003; Schäfer et al., 2006; Statheropoulos et al., 1998; Wehner and Wiedensohler, 2003; van der Zee et al., 1998). Statistical procedures like principal component analysis or cluster analysis represent helpful tools to gain an extended understanding of the meteorological effect on the spatial distribution of aerosols.

Up to now the majority of studies concerning aerosols and air quality are based on data at fixed stations. Measurements carried out during an emission experiment (Corsmeier et al., 2005) with extensive measurements on both sides of German motorway (Autobahn) showed a significant enhancement of PNC on the leeward side of a motorway while the change in mass was only marginally influenced by traffic emissions (Rosenbohm et al., 2005).

To examine the air quality in an extended area, a network of stationary measurement sites is needed. Substantial differences in the spatial aerosol distribution were observed between cities and their surroundings (Baltensperger et al., 2002; Boogaard et al., 2011; Harrison et al., 2012; Lenschow et al., 2001; Schäfer et al., 2011), but also in the cities themselves (Buzorius et al., 1999; Cyrys et al., 2008; Harrison et al., 2012; Johansson et al., 2007; Lenschow et al., 2001). However, such measurements always represent only the local conditions, which are usually influenced by emission sources. Due to the limited number of fixed stations, representative patterns of number and mass concentrations are hard to derive from these kinds of data sets. Even within urban areas particle concentrations show a high spatial variability (Puustinen et al., 2007).

Mobile measurements by means of moving devices (planes, trains, cars) are a prerequisite to avoid these disadvantages. Besides airborne measurements to study plumes (e.g. Corsmeier et al., 2002; Hasel et al., 2005; Junkermann et al., 2011a; Wieser, 2004), ground based mobile laboratories can be used for a broad range of applications (Kolb et al., 2004). With so-called “chasing experiments” the emissions of single vehicles under real-world operating conditions can be determined (e.g. Herndon et al., 2005; Pirjola et al., 2004). Furthermore, an assessment of emissions of the whole road traffic is possible (Pirjola et al., 2004; Wang et al., 2009; Weijers et al., 2004). Finally, mobile measurements are suitable to study the spatial variability of aerosols as well as other air quality parameters (Bukowiecki et al., 2002, 2003; Weimer et al., 2009).

The disadvantage of road-based vehicles is that the measurements always require human resources for operation. An alternative to avoid this is the usage of electric tramways during public transport services (Kehl, 2007). This gives the opportunity to carry out the measurement devices multiple times in a semi-automated manner and, in addition, along routes significant for population exposure to air pollution. A tramway track normally passes areas with different kinds of land use. Moreover, with a tram measurements are possible not only in traffic-exposed areas but also in traffic-free areas like pedestrian streets and, recreation areas but also in forests and agricultural zones.

In this study, we applied a tramway as a mobile platform for gaseous compounds, total number concentration and size distributions in the Karlsruhe region. Based on this data, in this study we addressed the following questions:

Are the spatial pattern of NO_x and PNCs similar?

Can we identify emissions sources other than traffic that cause high PNC?

How are the spatial distributions of PNC modified by wind direction, wind velocity and atmospheric stability?

2. The mobile laboratory: AERO-TRAM

We developed a mobile laboratory ‘AERO-TRAM’ for measurements of urban ground level pollutants. The instrument package is installed on an electric tramway of the municipal transport services of Karlsruhe (Verkehrsbetriebe Karlsruhe, VBK) in close collaboration with enviscope GmbH. Measurements were performed since end of 2009. The design allows fully automated measurements of aerosol parameters as particle number concentrations and particle size distributions. The gaseous components H_2O, O_3, NO, NO_x, CO and CO_2 are also provided. In addition, the ‘AERO-TRAM’ measures air temperature, relative humidity, air pressure and horizontal wind. The exact positions of the tram are obtained with an integrated global positioning system (GPS). A video camera at the front of the tramway records the environmental conditions (e. g. traffic situation, meteorological conditions like cloud cover or rain events) to support the data analysis interpretation. The operation on a vehicle with highly varying speed requires particular specifications of the sensors used. The analyzers were chosen to provide high quality measurements of pollutants in highly polluted areas as well as in slightly contaminated areas with only a background concentration. In order to obtain a high spatial resolution the temporal resolution of the sensors must be at least 10 s given by the maximum tramway velocity of 22 m s^{-1}, resulting in a maximum horizontal resolution of 220 m. Furthermore, the measurement setup must avoid self-contamination from the emissions of the tramway by abrasion from overhead line. The system has to work well under highly variable operation conditions on the tramway, especially regarding varying vibration conditions, electrical influences on the analyzers by the overhead contact line of the tramway, and long-term sensor stability for more than 1 year. The system must also operate properly under a widespread set of atmospheric conditions (e. g. temperatures between about +40 °C in summer and −20 °C in winter time. Safety regularities and the use of the tramway in the regular municipal transport cause additional limitations in the construction of the measurement system and the choice of analyzers (e. g. no radioactive sources are allowed). The automated measurement system has to be stand-alone for a minimum of four weeks (time between two inspections of the tramway), because of the limited access to the tramcar.

2.1. Design of the mobile laboratory and power supply

The selected mobile platform for the measuring system is a DUEWAG GT8-80C type tramcar (specifications: length 38.4 m; width

2.7 m; height 3.6 m; weight 51 tons; 117 seats and 126 standing places for passengers; year of construction 1989). A 750 V DC overhead line ensures the energy supply for the electrically driven tramcar. An indoor mounting of any measurement equipment associated with a loss of passenger capacity is not possible due to the fact that the tram is operated in regular municipal transport. So the measurement equipment is fully mounted on the roof. The limited space on the roof and installed tramcar operating technique demands a modular design of the measurement system existing of four communicating modules. A schematic overview is given in Fig. 1. Gas phase and particle analyzers are mounted in separate modules. The first module located at the front of the tramcar contains the inlet system for gas phase and particle measurements, particle analyzers, meteorological sensors and a video camera. In the second module the gas phase analyzers with an automated calibration device, GPS, and the administration and operating systems are embedded. In addition, an uninterrupted power supply unit (USV) including a battery package in case of short time power interruptions (up to 30 min) is installed in this module. These two modules are also air-conditioned to maintain stable service. Pressure cylinders containing the operation and calibration gases are placed in module three. A transducer located in the fourth module transforms the 750 V DC from the overhead contact line. The complete equipment has a weight of approximately 750 kg and consumes totaling 5 kW of power, including air conditioning.

2.2. Instrumentation

A full overview of the sensors for gaseous components, particles, meteorological parameters and position information is given in Table 1. The following details should be noted. Nitric oxide (NO) and nitrogen oxides (NO_x) are measured with two individual sensors. This allows a determination of nitrogen dioxide (NO_2) concentrations as difference between the two components. The low response time of 6 s makes the used optical particle counter (OPC) the most qualified analyzer for mobile measurement applications but in connection with a loss of information of the size distribution in lower size ranges. In future, a fast responding O_3 sensor (Zahn et al., 2012) will be additionally installed, basing on chemiluminescence reaction of O_3 and coumarin-47 according to Güsten et al. (1992).

2.3. The inlet system

Two separate inlet systems orientated towards the driving direction are mounted on the tramcar at a height of approximately

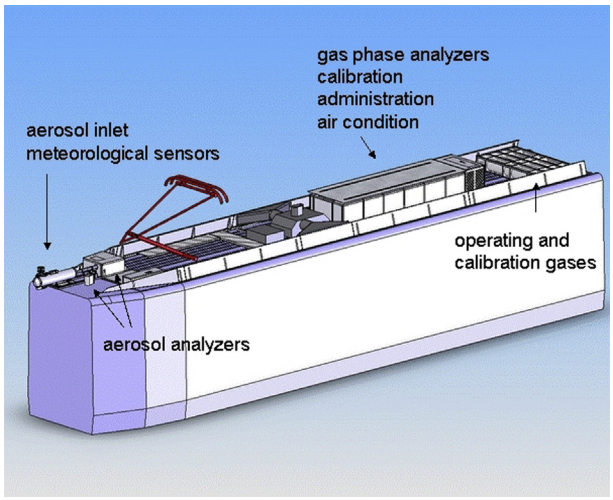

Fig. 1. Schematic overview of the design of the mobile measurement system 'AEROTRAM' on the roof of a tramcar.

3.5 m above the ground. At this height the influence of road dust emissions is minimized. Both inlets are located above the tramcar front end to catch the ambient air while driving before it is affected by the emissions from the pantograph and turbulence caused by the tramcar boundary layer. They are mounted close to each other (0.2 m) for a better analysis of the correlations between gas phase and particulate components. The inlet system material for the gas phase measurements is perfluoroalkoxy (PFA) for minimizing chemical reactions with the inlet walls and is equipped with a drop separator at the inlet port.

For the particle measurements a novel isokinetic inlet was developed (Klaus, 2009, Fig. 2). In contrast to other applications for mobile measurements, the design ensures an isokinetic air sampling not only at a fixed driving speed of the mobile platform but also for the entire speed range from 0 m s^{-1} to 22 m s^{-1} of the tramcar. The distance from the top of the particle inlet tube to the front of the tramcar is only 0.6 m. For high tramcar velocities the inlet will be slightly affected by the boundary layer of the tramcar, but the construction presents the best compromise between scientific requirements and safety regulations given by the municipal transport agency. The shroud around the front part of the particle inlet parallelizes the airflow at the inlet spike area leading to an isoaxial air sampling. Additionally, it serves as protection for the particle inlet and as mounting for the meteorological sensors. An adjustable pump ventilation at the end of the inlet system ensures that the velocity of the airflow inside the front part of the inlet tube correspond to the ambient, parallelized airflow. This ensures an isokinetic sampling. Otherwise, we would get an over-estimation of larger particles if the inside flow is lower (sub-isokinetic case) and an over-estimation of smaller particles if the inside flow is higher (super-isokinetic case), respectively. The ventilation is regulated by measurements of the airflow parallel to the aerosol inlet with an ultrasonic anemometer. The generated flow rate in the front inlet varies between 18.8 l min^{-1} and 302.6 l min^{-1} regarding the tramcar speed. However, for reliable particle measurements the flow rate to the analyzers and therefore the flow rate at the particle tap has to be constant at 18.8 l min^{-1}. For this, a diffuser widens the tube and reduces the flow velocity. To guarantee a controlled constant flow rate in the area of the particle tap, independent from the flow rates in the front part, the diffuser is movable along the tube axis resulting in an adjustable effective widening of the tube diameter. The air sample at the tap is surrounded by sheath air provided by a membrane pump (sample air to sheath air ratio 1:5) to avoid further particle losses. A further feature of the particle inlet system is the ability to measure the particle size distributions under dry conditions. For this purpose, the feeding tube with a length of 0.5 m between the OPC intake in the diffuser and the analyzer itself is made of Nafion (DuPont). The Nafion diffusion membrane provides a reduction of the water content of the particles. The tube length allows a significant reduction of relative humidity in the sample air compared to the atmosphere but misses the goal of a constant relative humidity. However, measurements of the particle size distributions at relative humidity under 50% are guaranteed apart from rain events. Particle losses due to diffusion of small particles ($d < 20$ nm) through the Nafion membrane are not considered because of the lower particle detection limit of the OPC of 250 nm.

Even the highly sophisticated inlet system cannot avoid particle loss. Therefore, analytical calculations of the collection efficiency were carried out. Particle loss processes due to (i) Brownian diffusion, (ii) sedimentation, and (iii) inertial impaction were considered (Klaus, 2009). It shows that major losses for particle diameters below 40 nm are caused by Brownian diffusion. For diameters above 1 μm however, the losses are mainly caused by sedimentation and inertial impaction. This yields a collection efficiency of

Table 1
Instrumentation of the 'AERO-TRAM'.

Module/Parameter	Measuring principle/Instrument type	Time resolution	Detection limit
Module 1 – aerosols & meteorology			
Total particle number 10 nm < D < 3 μm	Condensation particle counter (CPC)/TSI CPC 3772	3 s	10^4 particles cm^{-3}
Total particle number 4 nm < D < 3 μm	Condensation particle counter (CPC)/TSI CPC 3775	4 s	10^7 particles cm^{-3}
Size distribution 250 nm < D < 32 μm (31 size channels)	Optical particle counter (OPC)/GRIMM Dustmonitor 1.109	6 s	2000 particles cm^{-3} per size channel
Relative humidity	Capacitive thin film polymer sensor/VAISALA PTU 303	8 s	0–100%
Barometric pressure	Silicon capacitive absolute pressure probe/VAISALA PTU 303	2 s	500–1100 hPa
2-dimensional horizontal wind	Ultrasonic anemometer/GILL Windsonic	1 s	0–60 m/s
Air temperature	Platinum resistance thermometer PT100/VAISALA PTU 303		−40–60 °C
Traffic situation	Mobotix video camera		
Visible meteorological conditions			
Module 2 – Gas phase & GPS			
NO, NO_x	Chemiluminescence/ECO PHYSICS CLD 66 (NOx conversion with bluelight converter)	1 s	0.5 ppb
CO_2	IR absorption/LI-COR 7000	1s	0.1 ppm
H_20			0.1 g/kg
CO	Vaccum UV resonance fluorescence/Aerolaser AL 5001	1 s	2.5 ppb
O_3	UV absorption/Environnement O341M	6 s	1 ppb
Geographical information (longitude, latitude, altitude)	GPS μblox TIM-4H-0-000 on platine module RCB-4H ANTARIS 4		

over 90% for particle diameters between 3 nm and 2 μm at all driving conditions of the tramcar (Fig. 3).

2.4. Remote access and data storage

Due to the operational use of the tramcar in municipal transport the measurement system is only accessible during regular maintenance of the tramcar (approx. every four weeks). A remote access and telemetry system was used to allow online control of the system and online access to the data. There are two possibilities to communicate: (i) by WLAN for access from inside the tramcar and (ii) by UMTS for worldwide access (e. g. from office). Both communication paths are also used for transmission of the measurement data. As the connection is not online all the time, measurement data as well as status messages of the monitors and of the device (power status, flow rates, module temperatures, tramcar parameters like driving speed, door and coupling signals) are saved temporally and time synchronized on two industrial computers which are installed in both the particle module and the gas phase module. Independently from the response time of the air quality, analyzers and the meteorological sensors the measurement data is recorded every second with exception of the OPC whose sample rate corresponds to its time resolution (6 s). In addition, the computers automatically control the system, e. g controlled shutdown in the case of longer breaks of the tram. In case of failures of the device, the automatic control can be manually overridden via remote access.

2.5. Quality assurance and automatic calibration system

The measurement components are subject to particular calibration requirements due to the limited possibilities of accessing the analyzers. The two CPCs and the OPC have internal test routines to verify an error-free operation on start-up. A calibration of the particle analyzers during operation is not possible. Instead, an annual laboratory-based calibration is performed. The CO sensor is provided with an automated internal calibration routine. For the remaining gas phase analyzers (CO_2, NO, NO_x, O_3) an automated gas-mixing device was developed for calibration purposes. The mixing device provides defined concentrations within the calibration procedure. Zero air and certified calibration gases produce the individual calibration concentrations. The calibration gases are carried along in pressure cylinders with exception of O_3. An integrated O_3 generator produces this component. Zero air is made on

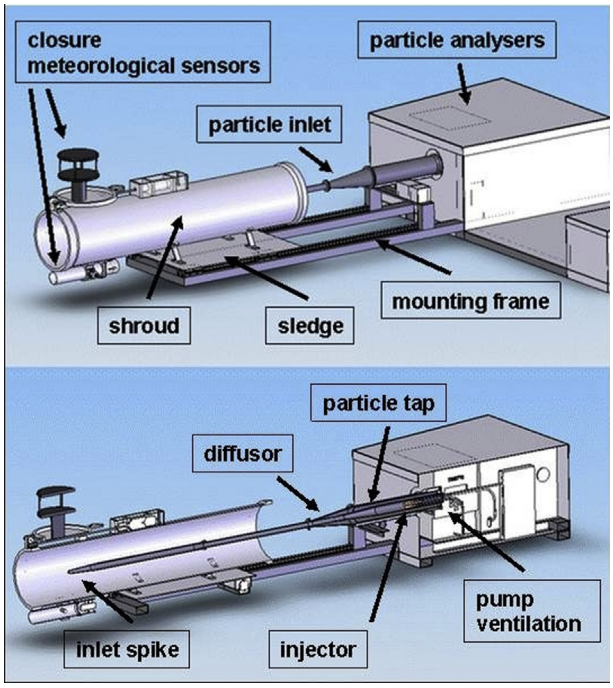

Fig. 2. Schematic overview of the design of the particle inlet. A movable sledge enables isokinetic probe sampling for different driving conditions of the 'AERO-TRAM'.

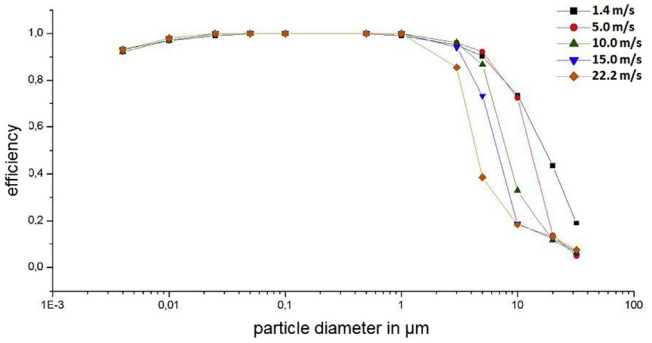

Fig. 3. Calculated overall efficiency of the particle inlet system at different tramcar velocities in dependence on the particle diameter (Klaus, 2009).

board from ambient air by means of scrubbers. The calibration routine is applied each night with zero air and three different concentrations including a span concentration (O_3 and NO: 200 ppb; NO_x: 400 ppb; CO_2: 500 ppm).

2.6. Selected tramcar routes

The rail network of Karlsruhe is characterized by a high density, covering the city of Karlsruhe, but also transits the surroundings up to locations 80 km outside the city. This offers the unique opportunity to study the air quality in highly polluted areas (e. g. near motorways, industry and at highly frequented crossroads) as well as in agricultural areas, forests, small settlements and pedestrian zones. In addition, a round-the-clock service operation allows a scientific analysis of diurnal, weekly or seasonal variations and in combination with a long-term use of the measurement system also a statistical analysis of the measurements.

The mobile laboratory runs on two different routes (Fig. 4a). The selection of the actual running line depends on the internal scheduling procedure of the municipal transport service. Line S1 links the Northern Black Forest southward of Karlsruhe (350 MSL), away from industry, to a village north of Karlsruhe (110 MSL), passing the inner city. This track is characterized by a specific height profile (Fig. 4b). The northern part and the transition of Karlsruhe are located in the Rhine Valley. Within a distance of 20 km the southern part of the track ascends towards the rural Northern Black Forest. The overall distance of the line is about 40 km and the tramway needs about 70 min for one run. Line S2 connects the western rural areas close to the Rhine trough the inner city with the rural areas in the northeast of Karlsruhe over a distance of 25 km. In contrast to line S1, this line is completely located in the Rhine Valley. Therefore the S2 has a complete flat profile (Fig. 4b). The run time of the tramway on this line is about 50 min. Both lines operate from the hinterland through the city center back into the hinterland and encounter different types of land use. They are crossing areas with very high concentrations of particles and trace gases as well as areas where only background concentrations are expected. In the city center of Karlsruhe both lines are using the same track for about 2 km. The orientation of the valley from southwest to northeast causes a well-known channeling of the large-scale flow (Fig. 4a). Within the valley southwesterly and northeasterly winds are prevailing (Groß and Wippermann, 1987; Kalthoff and Vogel, 1992; Vogel et al., 1986).

3. Data analysis

In this study we focused on the analysis of the air quality measurements of PNC and NO_x along the route S1 for the year 2010. We investigated regional differences of air pollutants concentrations as a central point. Within this year measurements were obtained from 2267 runs available on both lines. This includes both, drives on the complete routes and on parts. In total, a distance of 64305 km was covered in 2010. The total number of drives of only line S1 was 693 drives. Due to occasional device failures, 558 drives for PNC and 657 drives for NO_x were available.

We took only measurements into account when the tramcar was moving. This ensures that traffic emissions at crossroads during red light phases did not influence the data evaluation. Door opening during tram-stops at stations also affected the measurements by releasing air enriched with pollutants from inside the tramcar. Therefore, we also excluded data during the stops at stations.

We filtered the raw data for each separate measurement drive by calculating moving averages. As a result, the measurements were smoothed and regional differences in concentrations became

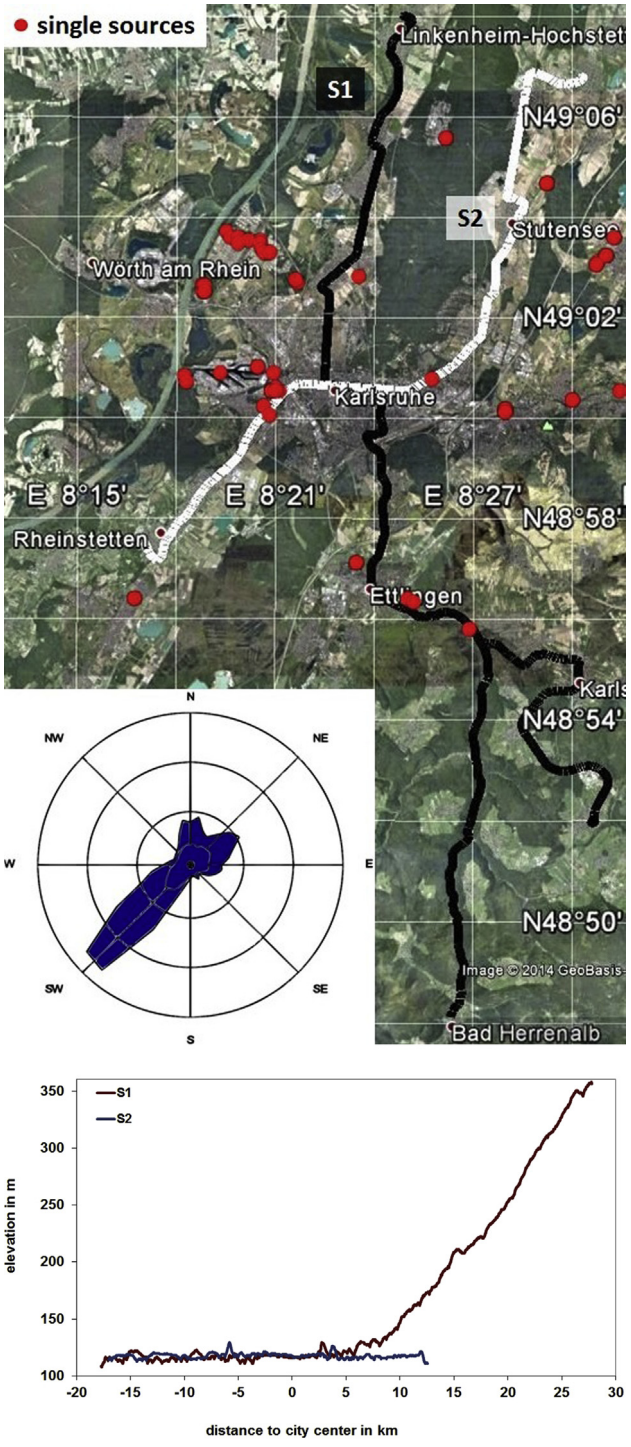

Fig. 4. a) Measuring routes of the 'AERO-TRAM' in the Karlsruhe area. Wind rose indicates the dominating wind directions in 2010. b) Corresponding height profiles relative to the city center.

clearer. As described above, measurements during halts of the tramcar are excluded with the effect that the resulting measurement data have several time lags. Consequently, moving quantities cannot be determined at a time interval but at a data point interval. We used an averaging over 60 data points which comes closest to an averaging over 1 min. For this interval, we calculated the central moving median $\tilde{c}_{.50}$, the 5 %- $\tilde{c}_{.05}$ and the 95 %-percentile $\tilde{c}_{.95}$ for each individual data point of the raw data. We used quantiles because these location parameters are robust

towards outliners. Malfunction of analyzers mainly caused these outliners.

The tramcar served not permanently the complete route during operation on line S1. Moreover it ran partially on a shorter leg. This leg is located between the northern terminal stop of line S1 (49° 8′ 0″ N, 8° 24′ 54″ E) and a stop in the town of Ettlingen south of Karlsruhe (48° 56′ 19″ N, 8° 24′ 33″ E) covering a distance of 27.1 km. It covers the city of Karlsruhe, its close suburban areas and the rural north. Thus, we focused on measurements on this part of the route. The combination resulted in 356 drives along this leg. For the evaluation in this study we had 285 drives for PNC and 342 drives for NO_x available.

In addition, we subdivided the considered part of the route into sections according to the land use (Fig. 5, Table 2). This facilitates the interpretation of the data. High pollution levels were expected to occur in densely populated areas like the inner city section E and the suburban sections D and F in the north and the south, respectively, of the urban area. Similar or even higher concentrations were expected at traffic-influenced locations such as the crossing of motorways (section C and G). Low concentrations were assumed to occur in the rural sections A and B where the route runs through small villages or along arable land.

3.1. Spatial patterns of PNC and NO_x

We binned the route of the considered leg into 542.50 m segments in order to analyze the spatial distributions of PNC and NO_x along the route. This size and the 1 s time resolution of the analyzers guarantees at least one measuring point within a section.

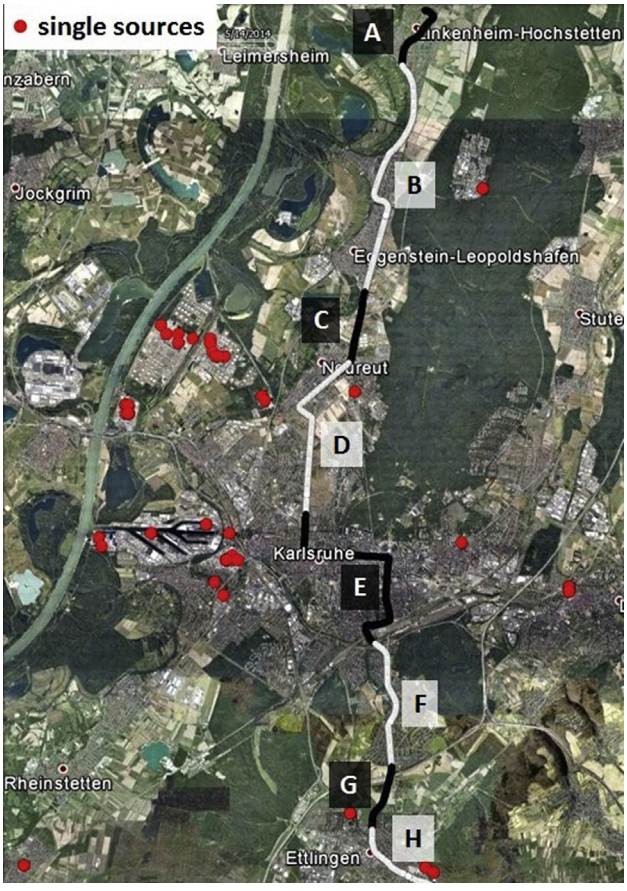

Fig. 5. Sectioned route of a shorter leg of line S1, investigated in this study (for details see Table 2).

Table 2
Area description of the sections along S1.

Section	Classification
A	Rural, settlement
B	Rural, settlement, agricultural areas
C	Motorway crossing (medium - heavy traffic), agricultural areas
D	Suburbs, grassy area, light traffic
E	City centre, busy crossroads, pedestrian zone
F	Suburbs, busy access road
G	Motorway crossing, agricultural areas
H	Small town, medium traffic, route often in distance to streets

Due to the varying tram velocity we get a significantly varying number of data points between some segments. As the tram only travels at high velocities in rural areas and away from human activities where no strong variation of pollutant concentrations occurs we think a smaller number is sufficient to represent typical results there. Next, we assigned the values of the derived moving quantiles $\tilde{c}$ to the according segments to determine the annual average distribution. The positioning was performed with the help of the GPS data. For each segment i the annual mean of the central moving median $\bar{\tilde{c}}_{.50,i}$, the 5 %-percentile $\bar{\tilde{c}}_{.05,i}$ and the 95 %-percentile $\bar{\tilde{c}}_{.95,i}$ of PNC and NO_x were calculated according to

$$
\begin{aligned}
\bar{\tilde{c}}_{.50,i,PNC} &= \frac{1}{N_{i,PNC}} \sum_{j=1}^{N_{i,PNC}} \tilde{c}_{.50,PNC,j},\\
\bar{\tilde{c}}_{.05,i,PNC} &= \frac{1}{N_{i,PNC}} \sum_{j=1}^{N_{i,PNC}} \tilde{c}_{.05,PNC,j},\\
\bar{\tilde{c}}_{.95,i,PNC} &= \frac{1}{N_{i,PNC}} \sum_{j=1}^{N_{i,PNC}} \tilde{c}_{.95,PNC,j},\\
\bar{\tilde{c}}_{.50,i,NO_x} &= \frac{1}{N_{i,NO_x}} \sum_{j=1}^{N_{i,NO_x}} \tilde{c}_{.50,NO_x,j},\\
\bar{\tilde{c}}_{.05,i,NO_x} &= \frac{1}{N_{i,NO_x}} \sum_{j=1}^{N_{i,NO_x}} \tilde{c}_{.05,NO_x,j},\\
\bar{\tilde{c}}_{.95,i,NO_x} &= \frac{1}{N_{i,NO_x}} \sum_{j=1}^{N_{i,NO_x}} \tilde{c}_{.95,NO_x,j}.
\end{aligned}
\tag{1}
$$

In this equations $N_{i,\mathrm{PNC}}$ and N_{i,NO_x} are the number of data j of the moving quantiles per segment i and for the year 2010. The spatial distribution of PNC averaged according to Eq. (1) for the year 2010 shows clear concentrations differences between the urban sections E to F and the rural northern sections A to D (Fig. 6a). The mean of the moving median $\bar{\tilde{c}}_{.50,PNC}$ of the particle number concentrations was generally higher in the city with values at around 15,000 cm^{-3}. The variations of the concentrations over the year, shown by the span between the mean of the moving 5 %-percentile $\bar{\tilde{c}}_{.05,PNC}$ and the mean of the 95%-percentile $\bar{\tilde{c}}_{.95,PNC}$, were higher by a factor of up to 2 than in the rural north. This was to be expected, since the density of emissions sources is higher, and emissions of particular pollutants and their precursors are larger in the city area than in the northern surroundings. Furthermore, the traffic density is higher and the distance of the measuring route to the nearest road is smaller.

The overall concentration profile in the city sections E and F is characterized by an inner part at a relative distance between −0.4 km and +4.4 km to the city center. There, the mean of the moving median $\bar{\tilde{c}}_{.50,PNC}$ was more or less constant at about 14,000 cm^{-3}. In this part of Karlsruhe the measuring route runs

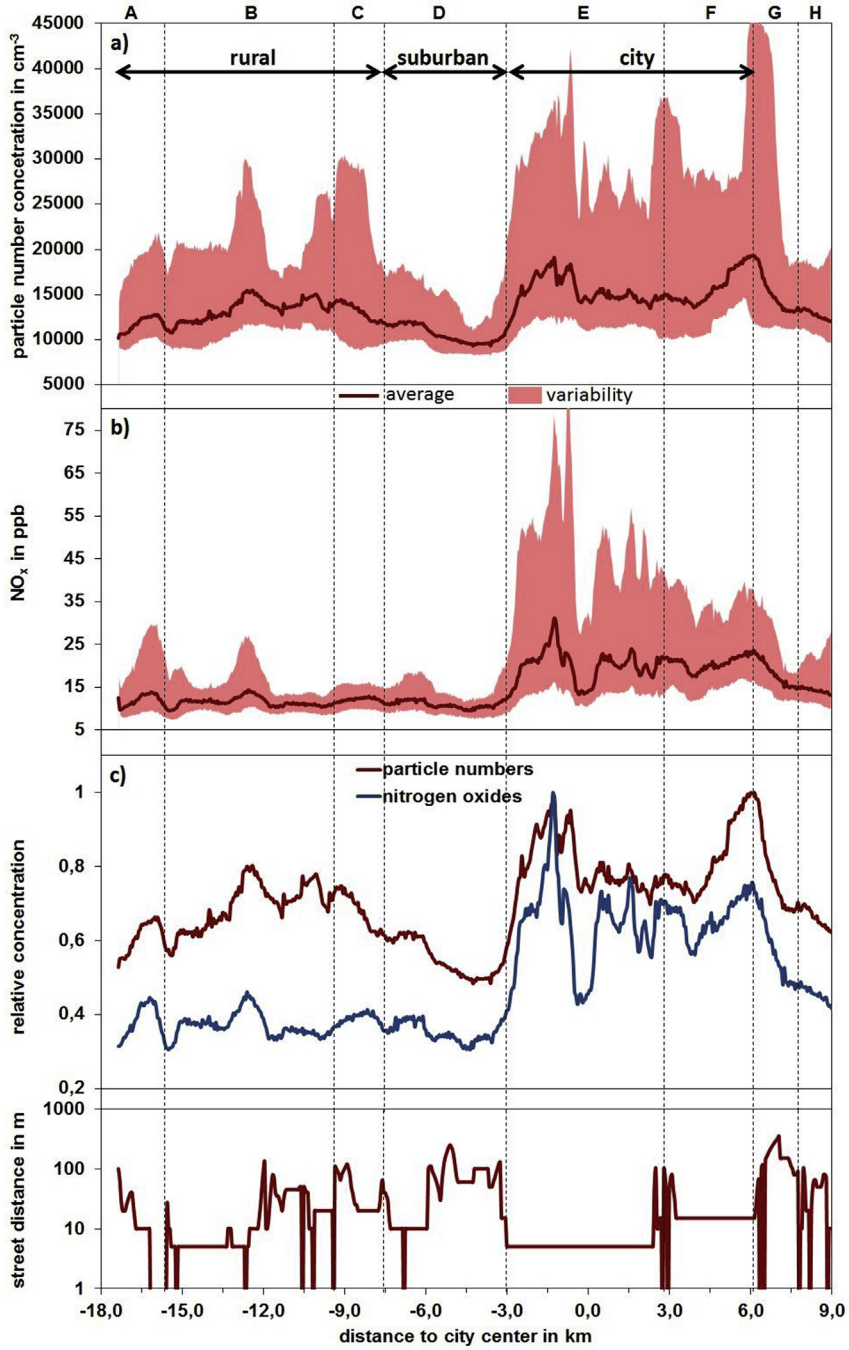

Fig. 6. Spatial distribution of particle numbers and NO_x along the investigated route. The lowest panel shows the distance of the measuring route to the nearest road. a) Annual mean of the moving median for particle number concentrations in 2010. Variability over the year is shown by the span between the annual mean of the moving 5% – and the 95% – percentile. b) Same but for NO_x – concentrations. c) Comparison of normalized profiles of both parameters demonstrates an increase of particle numbers with simultaneous constant NO_x – concentrations in rural section B.

through a pedestrian zone and along streets with relative low traffic density. The lack of traffic in the pedestrian zone (relative distance to the city center between −0.4 km and +0.1 km) caused appr. 1000 cm^{-3} lower values of $\bar{\bar{c}}_{.50,PNC}$ than in the rest of the inner part.

The higher values of $\bar{\bar{c}}_{.50,PNC}$ and the stronger variation at the edges of the inner part were associated with high levels of traffic there. The mean of the moving median $\bar{\bar{c}}_{.50,PNC}$ reached peak values of about 19,000 cm^{-3} at relative distances of −1.2 km and −0.6 km to the city center occur at busy main crossroads in the inner city (section E). We observed similarly high concentrations in the southern part of section F (relative distance of +6.1 km) at the crossing of a six-lane motorway. Occasionally, particle number concentrations reached values of $\bar{\bar{c}}_{.95,PNC}$ up to 40,000 cm^{-3} at these hotspots. The highest values of $\bar{\bar{c}}_{.95,PNC}$ are reached at the crossing of the motorway (relative distance of +6.1 km).

We also observed increased concentrations and variability at traffic-influenced locations in the northern surrounding although not with the same intensity. Traffic induced enhancements, in particular of $\bar{\bar{c}}_{.95,PNC}$, appeared at a crossing of a four lane motorway in section C (relative distance of −8.7 km) and at a grade crossing in section B (relative distance of −12.6 km). At this grade crossing waiting vehicles were responsible for the concentrations.

The concentration profile of the particle numbers along the northern part of measurement route (section A to D) showed two features. On the one hand, the mean of the moving median concentrations $\bar{\tilde{c}}_{.50,PNC}$ of about 12,000 cm^{-3} was significantly lower as in sections E and F. On the other hand $\bar{\tilde{c}}_{.50,PNC}$ is characterized by an inhomogeneous profile. Outside of the inner city section E the particle number concentrations dropped sharply in section D although this section is still within the city limits. The strong decline of the particle numbers was due to the fact that in section D the measurement route is further away from streets than in the sections E or F. The measurement route mostly passes meadows in this section. These two factors led to the strong decline of $\bar{\tilde{c}}_{.50,PNC}$ and the decreasing variation of PNC in section D.

With increasing distance to the city center a second rise of the mean of the moving median $\bar{\tilde{c}}_{.50,PNC}$ and the PNC variation occurred, in particular, in section B. This feature is quite remarkable, as the route is located in a rural environment there. In this section, the mean of the moving median of PNC showed comparable levels as the city sections E or F. In contrast to section D, the measurement route runs through a village in section B. The second increase of $\bar{\tilde{c}}_{.50,PNC}$ was most likely caused by the differing street distance and land use between section B and D. Based solely on these findings one might assume that the emissions from traffic but also from other local sources are stronger in section D. However, in the following we will show that this assumption is not true.

The annual mean spatial distribution of the nitrogen oxides concentrations did not indicate any concentration increase in the rural section B (Fig. 6b). The mean of the moving median $\bar{\tilde{c}}_{.50,NO_x}$ in this section were comparable of the other rural sections A and C and section D. Apart from this increase of PNC in section B the concentration profile of nitrogen oxides was very similar to the one of PNC. NO_x values of $\bar{\tilde{c}}_{.50,NO_x}$ and their variation were higher in the city section E to F than in the more rural sections A to D. Locations with enhanced values of $\bar{\tilde{c}}_{.50,NO_x}$ and variation, induced by traffic, correlate well with those of enhanced PNC. Compared to the city area, where the annual mean $\bar{\tilde{c}}_{.50,NO_x}$ was 20.2 ppb, the burden in the northern surroundings (section A–D) with 11.5 ppb was significant lower. Peak concentrations of up to 31.2 ppb of $\bar{\tilde{c}}_{.50,NO_x}$ occurred at a main crossroad in the inner city in section E (relative distance of −1.3 km to the city center) where values of $\bar{\tilde{c}}_{.95,NO_x}$ of up to 78.8 ppb were observed during 2010.

When we compared the concentration patterns of particle number and NO_x, it showed that the decline of NO_x in the northern surrounding was much stronger (Fig. 6c). The profiles of the mean of the moving median were normalized in respect to their individual maximum that occurred in both cases at a busy main crossroad in the inner city (relative distance of −1.2 km to the city center). While the nitrogen oxides showed a decline of about 70% in section D, the particle numbers decreased by 50% only. The different behavior of the concentration profiles in the remaining part of the northern surrounding is highlighted even more in Fig. 6c. Nitrogen oxides concentrations remained more or less constant for the rest of the route (section A to C) while at the same time the particle numbers increased again in section B up to 80% of the inner city maximum. This means that the second increase of particle numbers could not originate from local sources like traffic and there must have been other reasons.

3.2. Source appointment of high PNC in the rural north

We applied a cluster analysis to investigate the influence of meteorology on the spatial distribution of PNC. In detail, we were interested on the impact of the parameters wind direction, wind speed and boundary layer stability. The clustering was based on measurements at the meteorological 200 m-tower of the Institute for Meteorology and Climate Research (IMK), 10 km north of Karlsruhe center (49° 5′ 33′′ N, 8° 25′ 33′′ E, 110.4 MSL). The mast is highly instrumented with meteorological sensors at different heights (Kalthoff and Vogel, 1992; Barthlott and Fiedler, 2003). We thus used an individual point measurement to determine the impact of the above-mentioned meteorological parameters on the spatial distribution of PNC. Kalthoff and Vogel (1992) showed that measurements of the wind direction in 200 m height represent well the large-scale situation. We therefore assumed the same for the wind velocity measurements in 200 m height. We consequently did not account for small-scale effects of the spatial distribution of the meteorological parameters on the particle concentrations. We used 10-min means of measurements of wind direction and wind speed at a height of 200 m. Measurements of the wind direction but at 100 m were used to calculate the stability classes. The stability is classified by the six dispersion classes of Pasquill (1961). The classes itself are routinely determined by the standard deviation of the wind direction measurements within a 10-min interval (Blackadar, 1997). We summed up the classes of unstable conditions A to C and, respectively, of stable conditions E and F to one individual class. The neutral class remained unchanged. To study the influence on the spatial distribution of PNC, we introduced three groups of clusters. We assigned data of an individual measurement drive to a certain cluster, if 75% of the driving time met the particular criterion.

The first group contained two clusters for winds with a southern and northern component. We chose these two directions, according to the dominating wind directions in our study area (Fig. 4a). 110 drives during northerly winds and 142 drives during southerly winds were available. The second group contained two clusters of southerly winds with two different velocities. One cluster includes measurements during low velocities (1–5 m s^{-1}) from 38 drives, the other high velocities (>5 m s^{-1}) from 84 drives. The last group comprehended three clusters for stable (34 drives), neutral (81 drives), and unstable conditions (102 drives). For all of this clusters we calculated $\bar{\tilde{c}}_{.50,PNC}$ according to Eq. (1).

Fig. 7a shows the influence of the wind direction on the spatial distribution of PNC The particle numbers in the inner city (section E) and the rural sections D indicated almost no dependence on wind direction. We found one exception where the route was located downwind of a local emission source during northerly winds. In this case there was a motorway in the north of the measuring route and is located in section F at a relative distance of 3.0 km from the city center. There we observed clearly higher particle numbers in section F during northerly winds. The advection of particle emissions originating from the nearby motorway lead to 40% higher particle concentrations for the north wind case. The most remarkable feature occurred in section B. There, we observed up to 30% higher values of $\bar{\tilde{c}}_{.50,PNC}$ during southerly winds compared to the concentrations during northerly winds.

When we treated the annual mean of the spatial pattern of PNC in Section 3.2 we found a second increase of $\bar{\tilde{c}}_{.50,PNC}$ in the same section. This increase, in addition, occurred only during southerly winds and led to particle numbers up to 17,000 cm^{-3}. For northerly winds, $\bar{\tilde{c}}_{.50,PNC}$ was with 13,000 cm^{-3} at the same levels in the rural north area of Karlsruhe (sections A to D), besides a concentration enhancement at a smaller motorway in section C. During northerly winds here the route is located downwind of this motorway. Based on these findings it becomes clear that the enhanced concentrations cannot be attributed to local sources. Moreover, we identified an industrial area including refineries (15.5 Mt/a capacity) 5 km away and a 550 MW coal power plant in a distance of appr. 10 km to be the main sources for these high concentrations (Fig. 8). In addition, we derived the Ångström exponent $\alpha_{440-870nm}$ from measurements of our AERONET station (Holben et al., 1998; Dubovik and King, 2000) near the meteorological tower and 2 km

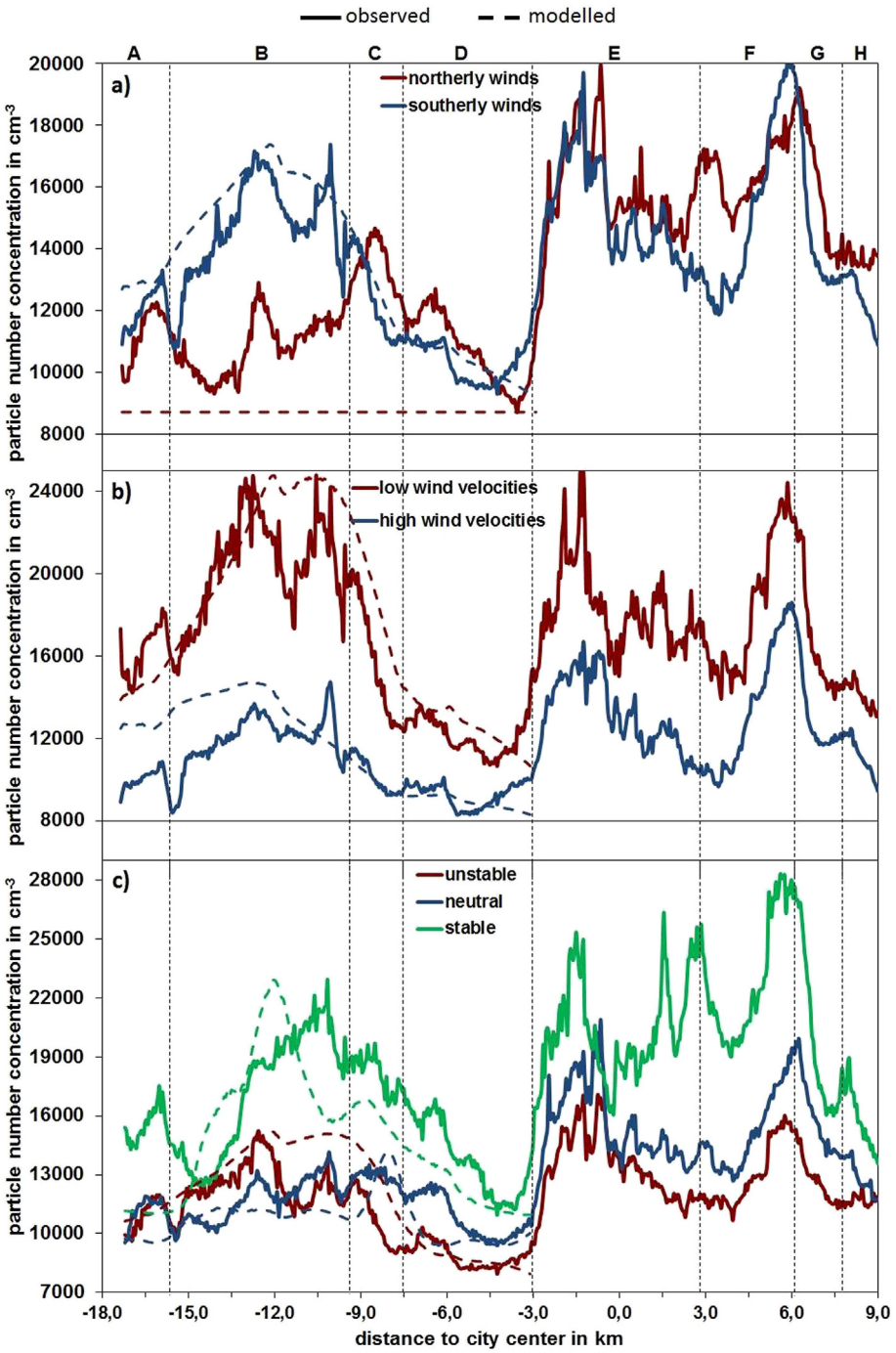

Fig. 7. Spatial distribution of particle numbers influenced by meteorological parameters. a) Second particle increase in rural section B only occurs during southerly wind directions. b) Increase is more pronounced for low wind speeds during southerly winds and as high as in inner city section E. c) Significant enhancement of particle numbers in section B during stable stratification.

away from the measurement route. We took into account AERONET measurements of $\alpha_{440-870nm}$ for operating days of the AERO-TRAM averaged over the year. We found a higher Ångström exponent ($\alpha_{440-870nm} = 1.72$) for southerly winds than for northerly winds ($\alpha_{440-870nm} = 1.43$). This indicates an increase of smaller particles during events when industrial emissions affect particle numbers in the rural north of Karlsruhe. As mentioned before the orientation of the Rhine Valley leads to a deflection of winds with southern components to southwesterly winds. Therefore, the industrial emissions of particulate pollutants or their gaseous precursors are transported in direction of section B. Recent studies (Fernández-Camacho et al., 2012; Junkermann et al., 2011a; 2011b) indicate that industrial emissions can be a source for ultrafine particles with implications for the surroundings. These particles can be either emitted directly but also be formed within the plume despite of emission regulations.

This hypothesis was confirmed when we compared the second group of clusters. The mean of the moving median $\bar{\tilde{c}}_{.50,PNC}$ is generally higher for low velocities than for high velocities during southerly winds. This is illustrated in Fig. 7b, showing the comparison between $\bar{\tilde{c}}_{.50,PNC}$ of the clusters for low and high wind velocities. The influence of wind velocity on particle numbers varied,

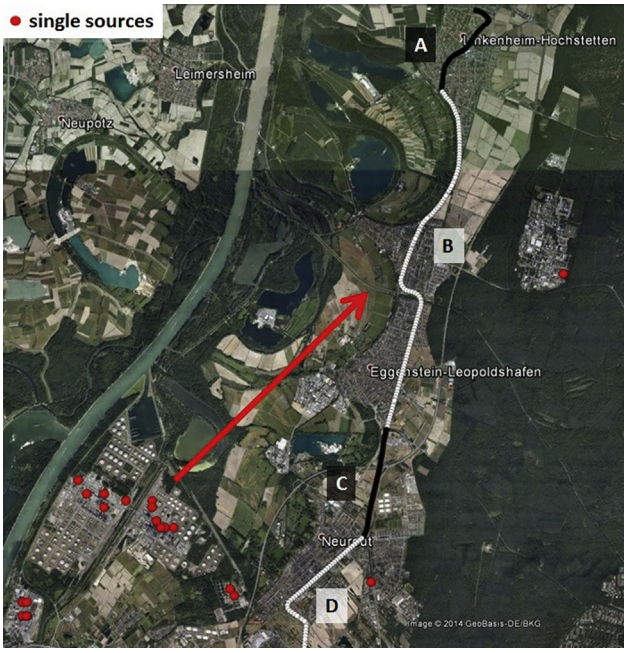

Fig. 8. Identified sources in an industrial area, leading to second particle number increase in rural section B. Red arrow highlights the dominating southwesterly wind direction in the domain. (For interpretation of the references to colour in this figure legend, the reader is referred to the web version of this article.)

however, spatially. In urbanized areas (section D–F) with dominating area sources the concentration differences due to different wind velocities are in the order of 30–50%. In contrast, the influence of elevated sources in the rural section B leads to changes in the particle number concentration in the order of 100%.

Concerning the rural enhancement of particle numbers due to industrial emissions, we observed for both clusters the second increase in section B. Wind velocities between 1 and 5 m s^{-1} caused particle number concentration of up to 25,000 cm^{-3} in section B. These numbers are comparable with the particle numbers in the inner city (section E). The increase is with 14,000 cm^{-3} not so distinct for velocities greater than 5 m s^{-1} as the dilution of pollutants in the atmosphere is more pronounced for high wind speeds. Furthermore, AERONET measurements suggest a higher amount of small particles during conditions with low wind velocities ($\alpha_{440-870nm} = 1.73$) than for high velocities ($\alpha_{440-870nm} = 1.59$).

The last group of clusters, regarding boundary layer stability, validated also our findings that the air quality in the rural section B is influenced by industrial emissions. Fig. 7c indicates the different concentration profiles of $\bar{\bar{c}}_{.50,PNC}$ for the three stability classes. Particle number concentrations along the route were lowest during unstable boundary layer conditions (red profile) but very similar during neutral boundary layer conditions (blue profile). During stable conditions (green profile), with generally lower wind speeds than in the other two cases, the particle pollution was significantly higher along the route. Furthermore, we observed a more clearly pronounced second particle increase in section B for stable conditions. There, concentrations were with up to 23,000 cm^{-3} significantly higher than in the adjacent section A, C and D in contrast to the other stability classes. For the other classes, particle numbers of up to 14,000 cm^{-3} occurred in section B. In combination with assumption of a prevailing southwestern wind direction during stable boundary layer conditions a clear modification of the air quality in section B by industrial plants in the southwestern vicinity can be expected. However, it must be mentioned, that for this cluster group only a small number of drives were available. This is especially the case for drives during stable stratification.

To underline these findings we determined the impact of the industrial emissions applying a Gaussian plume model.

We used sigma parameters of Klug (1969) to calculate the concentration distribution for each individual cluster at ground level. Two emissions sources were considered located in the southwestern vicinity. One is a coal fired power plant the second are installations belonging to a refinery. In the refinery area we found two main stacks and for simplification we combined them into one single source. Both, the power plant and the refinery stacks have a height of approx. 220 m and source strengths of about 335 kg h^{-1} and 885 kg h^{-1}, respectively of particulate substances and precursors. The emission data was taken from the emission registry of the Germany Federal Environmental Agency (PRTR, 2014). To determine the effective source height we used plume rise formulas of Briggs (1969). Information about stack diameter and exit velocity, as well as exit temperature and ambient temperature at stack height of the two emission sources were not available. In order to determine the buoyancy flux parameters we assumed a stack diameter of 15 m and an ambient temperature of 10.7 °C at stack height. This temperature corresponds to the long-term average in Karlsruhe. In addition, we used data about stack exit velocity (power plant: 10 m s^{-1}, refinery: 7 m s^{-1}) and temperature (100 °C and 200 °C, respectively) of Pregger and Friedrich (2009) for coal power plants with more than 1.000 MW and for refineries. The resulting buoyancy flux parameters were 1320 m^4 s^{-3} for the power plant and 1545 m^4 s^{-3} for the refinery.

In order to calculate the sigma parameters we used Pasquill stability classes routinely determined at our meteorological tower as described in Section 3.2. Wind speed and wind direction measured at the tower at a height of 200 m were used as input data for the Gaussian plume model for each of the individual clusters. Calculations were carried out for periods when tram measurements were performed. For the stability clusters presented in Fig. 7c calculations were only carried out for southerly winds.

We subsequently determined the mean distribution of concentrations $\bar{c}_{i,gauss}$ over all calculated distributions along the 50 m segments of the measurement route between section A and D (segments 1–287) for each cluster. To compare model results and measurements we normalized $\bar{c}_{i,gauss}$ according to

$$\bar{\bar{c}}_{i,gauss} = \left[\bar{c}_{i,gauss} - \min_{1\le i\le 287} \bar{c}_{i,gauss}\right] \cdot \frac{\max_{1\le i\le 287} \bar{\bar{c}}_{.50,i,PNC} - \min_{1\le i\le 287} \bar{\bar{c}}_{.50,i,PNC}}{\max_{1\le i\le 287} \bar{c}_{i,gauss} - \min_{1\le i\le 287} \bar{c}_{i,gauss}} + \min_{1\le i\le 287} \bar{\bar{c}}_{.50,i,PNC} \quad (2)$$

where $\bar{c}_{i,gauss}$ and $\bar{\bar{c}}_{.50,i,PNC}$ comes from the same cluster. This normalization was necessary as simple Gaussian model is not ably to take into account aerosol dynamics. In addition, applying this normalization we can take into account varying background concentrations between the clusters and the effects smaller area sources which are both not considered in the Gaussian model.

Compared to our measurements the calculated distribution along the route showed generally a good agreement. This confirms the influence of elevated sources on the particle pollution in sections A–D.

The calculated particle concentrations for southerly winds (Fig. 7a) clearly indicate that they are influenced by the two industrial emission sources. Again the spatial patterns simulated with the Gaussian plume model correlate quite well with the observed ones.

Considering the effect of wind velocity (Fig. 7b) the calculated particle numbers along the route also shows clear contrasts induced by the two different wind velocities and a good accordance between model and observations. Low wind velocities during southerly winds leads to a steep increase of concentrations within sections B and C. The impact of the two main sources is quite clear. During conditions with high wind velocities the enhancement is also noticeable but not so significant. The increase is not so steep but wider. We ascribe this to a stronger dilution effect during higher wind velocities resulting in smaller concentration differences in this section.

The Gaussian plume model calculation for the stability class clusters (Fig. 7c) also indicates a clear impact of the industrial emissions on the particle pollution in the rural north. For stable conditions the calculated effective source heights led to unrealistic results. Therefore, we assumed a constant height of 260 m. The concentration profile for stable conditions is slightly displaced but reproduces generally the observations. For the other remaining stratification cases, where we considered again the determination of the source height according to Briggs (1969), the profiles are in good accordance with the measurements. The calculated profile for stable conditions shows a narrower and steeper profile than for the other cases. We attribute this to a more linear dispersion of the industrial plumes during stable conditions.

4. Summary and conclusions

By developing and operating the innovative measurement device “AERO-TRAM”, spatial distributions of air quality parameters for an agglomeration area in Germany were extensively monitored. We showed that the “AERO-TRAM” provides temporally and spatially high-resolved mobile measurements during regular operations of a tramcar in municipal transport services. We demonstrated that the observation system is a suitable tool to determine concentrations of particulate and gaseous pollutants by an independent and almost automatic measurement system. Data is collected regularly since the end of 2009 until end of 2011. More than 2200 measurement drives were available for the year 2010. The ability to operate not only in the city of Karlsruhe but also in the northern and southern surroundings allows studying air pollution under quite different emission conditions.

Analysis of the measurement data for the year 2010 provided a spatially highly resolved picture of the annual average distribution of particle number and nitrogen oxides concentrations. We found particle number concentrations of 15,000 cm^{-3} on average and a higher variability of the concentrations in the inner city. In the rural surroundings we observed mean concentrations 12,000 cm^{-3} and a lower variability over the year. Highest annual mean concentrations of up to 19,000 cm^{-3} occurred at traffic influenced locations. There, values up to 40,000 cm^{-3} were attained over the year. In case of NO_x we found concentrations of 20 ppb in the inner city, 10 ppb in the rural surroundings, and up to 30 ppb at traffic influenced locations.

We noticed a generally good correlation between particle number and NO_x concentrations along the route, in particular at traffic-influenced locations. We found, however, to some extent significant differences in gradients between city and rural concentrations. A decline of 70% in case of NO_x was observed in contrast to 50% for PNC. Furthermore, particle numbers increased again to 80% in the rural surroundings in comparison to the inner city maximum of PNC while nitrogen oxides levels stayed on 50%. As a correlation between particle numbers and nitrogen oxides did not occur there local emission sources like traffic cannot be responsible for the remarkable high particle number concentrations in this rural area.

Cluster analysis revealed a clear influence of the meteorological parameters wind direction, wind speed and boundary layer stability on the concentration profiles of particle number, in particular for the rural area where a second increase of PNC was observed. This increase only occurred during southwesterly winds and is most pronounced in combination with low wind speed conditions between 1 m s^{-1} and 5 m s^{-1}. The increase could be most probably linked to emissions of industrial plants in the southwestern vicinity of the rural area. This assumption was confirmed by Gaussian plume model calculations. The consideration of boundary layer stability also indicated a significant influence on the profile of PNC. Stable boundary layer conditions lead to considerably higher concentration along the route than for unstable or neutral cases. The second particle number increase in the rural area was particularly recognizable during stable conditions when normally low wind speeds are prevailing. These findings strengthen the assumption that the particulate pollution this particular area is affected significantly by industrial emissions from the vicinity. Our study showed that under certain meteorological conditions, particulate concentrations were enhanced up to 40% in this area.

Acknowledgments

Funding of the ‘AERO-TRAM’ project was provided by Baden-Wuerttemberg Research Program Securing a Sustainable Living Environment (BWPLUS) under project number BWU 27003. We would like to thank Rolf Maser, Dr. Dieter Schell and Christoph Klaus of enviscope GmbH for the support in developing and constructing the isokinetic inlet and the measurement system. We are also very grateful for the supply of the tramcar by the municipal transport services of Karlsruhe (VBK). In particular, special thanks to Dr. Walter Casazza, Alexander Wetzel and Matthias Schreiber.

References

Baltensperger, U., Streit, N., Weingartner, E., Nyeki, S., Prévôt, A., Van Dingenen, R., Virkkula, A., Putaud, J.-P., Even, A., ten Brink, H., Blatter, A., Neftel, A., Gäggeler, H., 2002. Urban and rural aerosol characterization of summer smog events during the PIPAPO field campaign in Milan, Italy. J. Geophys. Res. 107 (D22), 8193.

Barthlott, C., Fiedler, F., 2003. Turbulence structure in the wake region of a meteorological tower. Bound.-Lay. Meteorol. 108 (1), 175–190.

Blackadar, A.K., 1997. Turbulence and Diffusion in the Atmosphere: Lectures in Environmental Sciences. Springer, Berlin.

Boogaard, H., Kos, G., Weijers, E., Janssen, N., Fischer, P., van der Zee, S., de Hartog, J., Hoek, G., 2011. Contrast in air pollution components between major streets and background locations. Particulate matter mass, black carbon, elemental composition, nitrogen oxide and ultrafine particle number. Atmos. Environ. 45 (3), 650–658.

Brunekreef, B., Holgate, S., 2002. Air pollution and health. Lancet 360 (9341), 1233–1242.

Briggs, G.A., 1969. Optimum formulas for Buoyant plume rise. Phil. Trans. R. Soc. A. 165, 197–203.

Bukowiecki, N., Dommen, J., Prévôt, A., Richter, R., Weingartner, E., Baltensperger, U., 2002. A mobile pollutant measurement laborator – measuring gas phase and aerosol ambient concentrations with high spatial and temporal resolution. Atmos. Environ. 36 (36–37), 5569–5579.

Bukowiecki, N., Dommen, J., Prévôt, A., Weingartner, E., Baltensperger, U., 2003. Fine and ultrafine particles in the Zürich (Switzerland) area measured with a mobile laboratory. An assessment of the seasonal and regional variation throughout a year. Atmos. Chem. Phys. 3 (5), 1477–1494.

Buzorius, G., Hämeri, K., Pekkanen, J., Kulmala, M., 1999. Spatial variation of aerosol number concentration in Helsinki city. Atmos. Environ. 33 (4), 553–565.

Corsmeier, U., Kalthoff, N., Vogel, B., Hammer, M.-U., Fiedler, F., Kottmeier, C., Volz-Thomas, A., Konrad, S., Glaser, K., Neininger, B., Lehning, M., Jaeschke, W., Memmesheimer, M., Rappenglück, B., Jakobi, G., 2002. Ozone and PAN formation inside and outside of the Berlin plume – process analysis and numerical process simulation. J. Atmos. Chem. 42 (1), 289–321.

Corsmeier, U., Kohler, M., Vogel, B., Vogel, H., Fiedler, F., 2005. BAB II: a project to evaluate the accuracy of real-world traffic emissions for a motorway. Atmos. Environ. 39 (31), 5627–5641.

Cyrys, J., Pitz, M., Heinrich, J., Wichmann, H.-E., Peters, A., 2008. Spatial and temporal variation of particle number concentration in Augsburg, Germany. Sci. Total Environ. 401 (1–3), 168–175.

Dubovik, O., King, M.D., 2000. A flexible inversion algorithm for retrieval of aerosol optical properties from sun and sky radiance measurements. J. Geophys. Res. 105, 20673–20696.
EC, 11.6.2008. Directive 2008/50/EC of the European Parliament and of the Council of 21 May 2008 on ambient air and cleaner air for Europe. Off. J. Eur. Union L152 (Brussels).
Fernández-Camacho, R., Rodríguez, S., de la Rosa, J., Sánchez de la Campa, A.M., Alastuey, A., Querol, X., González-Castanedo, Y., Garcia-Orellana, I., Nava, S., 2012. Ultrafine particle and fine trace metal (As, Cd, Cu, Pb and Zn) pollution episodes induced by industrial emissions in Huelva, SW Spain. Atmos. Environ. 61, 507–517.
Gomišček, B., Hauck, H., Stopper, S., Preining, O., 2004. Spatial and temporal variations of PM1, PM2.5, PM10 and particle number concentration during the AUPHEP – project. Atmos. Environ. 38 (24), 3917–3934.
Groß, G., Wippermann, F., 1987. Channelling and countercurrent in the Upper Rhine Valley: numerical Simulations. J. Clim. Appl. Meteorol. 26 (10), 1293–1304.
Güsten, H., Heinrich, G., Schmidt, R., Schurath, U., 1992. A novel ozone sensor for Direct eddy flux measurements. J. Atmos. Chem. 14 (1–4), 73–84.
Harrison, R., Laxen, D., Moorcroft, S., Laxen, K., 2012. Processes affecting concentration of fine particulate matter (PM2.5) in the UK atmosphere. Atmos. Environ. 46, 115–124.
Hasel, M., Kottmeier, C., Corsmeier, U., Wieser, A., 2005. Airborne measurements of turbulent trace gas fluxes and analysis of eddy structure in the convective boundary layer over complex terrain. Atmos. Res. 74 (1–4), 381–402.
Herndon, S., Jayne, J., Zahniser, M., Worsnop, D., Knighton, B., Alwine, E., Lamb, B., Zavala, M., Nelson, D., Barry McManus, J., Shorter, J., Canagaratna, M., Onasch, T., Kolb, C., 2005. Characterization of urban pollutant emission fluxes and ambient concentration distributions using a mobile laboratory with rapid response instrumentation. Faraday Discuss. 130, 327–339.
Holben, B.N., Eck, T.F., Slutsker, I., Tanre, D., Buis, J.P., Setzer, A., Vermote, E., Reagan, J.A., Kaufman, Y., Nakajima, T., Lavenu, F., Jankowiak, I., Smirnov, A., 1998. AERONET – a federated instrument network and data archive for aerosol characterization. Remote Sens. Environ. 66, 1–16.
Johansson, C., Norman, M., Gidhagen, L., 2007. Spatial & temporal variations of PM10 and particle number concentrations in urban air. Environ. Monit. Assess. 127 (1–3), 477–487.
Junkermann, W., Hagemann, R., Vogel, B., 2011a. Nucleation in the Karlsruhe plume during the COPS/TRACKS – Lagrange experiment. Quart. J. Roy. Meteor. Soc. 137 (S1), 267–274.
Junkermann, W., Vogel, B., Sutton, M.A., 2011b. The climate penalty for clean fossil fuel combustion. Atmos. Chem. Phys. 11, 12917–12924.
Kalthoff, N., Vogel, B., 1992. Counter-current and channeling effect under stable stratification in the area of Karlsruhe. Theor. Appl. Climatol. 45 (2), 113–126.
Kampa, M., Castanas, E., 2008. Human health effects of air pollution. Environ. Pollut. 151 (2), 362–367.
Katsouyanni, K., 2003. Ambient air pollution and health. Br. Med. Bull. 68 (1), 143–156.
Kehl, P., 2007. GPS based Dynamic Monitoring of Air Pollutants in the City of Zürich, Switzerland. Dissertation, ETH Zürich.
Klaus, C., 2009. Entwicklung eines isokinetischen Einlasssystems autonomen Langzeitmessung von Aerosolen auf dem Dach einer Straßenbahn, p. 92. Diploma thesis, Fachhochschule Wiesbaden, Wiesbaden, Germany.
Klug, W., 1969. Ein Verfahren zur Bestimmung der Ausbreitungsbedingungen aus synoptischen Beobachtungen. Staub-Reinhaltung Luft 29 (4), 143–147.
Kolb, C.E., Herndon, S., Barry McManus, J., Shorter, J., Zahniser, M., Nelson, D., Jayne, J., Canagaratna, M., Worsnop, D., 2004. Mobile laboratory with rapid response instruments for real-time measurements of urban and regional trace Gas and particulate distributions and emission source characteristics. Environ. Sci. Technol. 38 (21), 5694–5703.
Künzli, N., Kaiser, R., Medina, S., Studnicka, M., Chanel, O., Filliger, P., Herry, M., Horak Jr., F., Puybonnieux-Texier, V., Quénel, P., Schneider, J., Seethaler, R., Vergnaud, J.-C., Sommer, H., 2000. Public-health impact of outdoor and traffic-related air pollution: a European assessment. Lancet 356 (9232), 795–801.
Lenschow, P., Abraham, H., Kutzner, K., Lutz, M., Preuß, J., Reichenbächer, W., 2001. Some ideas about the sources of PM10. Atmos. Environ. 35 (1), 23–33.
Liu, L., Breitner, S., Schneider, A., Cyrys, J., Brüske, I., Frank, U., Schlink, U., Leitte, A.M., Herbarth, O., Wiedensohler, A., Wehner, B., Pan, X., Wichmann, H.-E., Peters, A., 2013. Size-fractioned particulate air pollution and cardiovascular emergency room visits in Beijing, China. Environ. Res. 121, 52–63.
Pasquill, F., 1961. The estimation of the dispersion of windborne material. Met. Mag. 90 (1063), 33–49.
Penttinen, P., Timonen, K., Tiittanen, P., Mirme, A., Ruuskanen, J., Pekkanen, J., 2001. Ultrafine particles in urban air and respiratory health among adult asthmatics. Eur. Respir. J. 17 (3), 428–435.
Pirjola, L., Parviainen, H., Hussein, T., Valli, A., Hämeri, K., Aaalto, P., Virtanen, A., Keskinen, J., Pakkanen, T., Mäkelä, T., Hillamo, R., 2004. "Sniffer" – a novel tool for chasing vehicles and measuring traffic pollutants. Atmos. Environ. 38 (22), 3625–3635.
Pöschl, U., 2005. Atmospheric aerosols: composition, transformation, climate and health effects. Angew. Chem. Int. Ed. 44 (46), 7520–7540.
Pope, C., Burnett, R., Thun, M., Calle, E., Krewski, D., Ito, K., Thurston, G., 2002. Lung cancer, cardiopulmonary mortality, and long-term exposure to fine particulate air pollution. J. A. Med. Inf. Assn. 287 (13), 1132–1141.
Pregger, T., Friedrich, R., 2009. Effective pollutant emission heights for atmospheric transport modelling based on real-world information. Environ. Pollut. 157 (2), 552–560.
PRTR, 2014. Deutsches Schadstofffreisetzungs- und -ungsregister, Umweltbundesamt. www.thru.de.
Puustinen, A., Hämeri, K., Pekkanen, J., Kulmala, M., de Hartog, J., Meliefste, K., ten Brink, H., Kos, G., Katsouyanni, K., Karakatsani, A., Kotronarou, A., Kavouras, I., Meddings, C., Thomas, S., Harrison, R., Ayresi, J., van der Zee, S., Hoek, G., 2007. Spatial variation of particle number and mass over four European cities. Atmos. Environ. 41 (31), 6622–6636.
Rosenbohm, E., Vogt, R., Scheer, V., Nielsen, O., Dreiseidler, A., Baumbach, G., Imhof, D., Baltensperger, U., Fuchs, J., Jaeschke, W., 2005. Particulate size distributions and mass measured at a motorway during the BAB II campaign. Atmos. Environ. 39 (31), 5696–5709.
Schäfer, K., Emeis, S., Hoffmann, H., Jahn, C., 2006. Influence of mixing layer height upon air pollution in urban and sub-urban areas. Meteor. Z. 15 (6), 647–658.
Schäfer, K., Emeis, S., Schrader, S., Török, S., Alföldy, B., Osan, J., Pitz, M., Münkel, C., Cyrys, J., Peters, A., Sarigiannis, D., Suppan, P., 2011. A measurement based analysis of the spatial distribution, temporal variation and chemical composition of particulate matter in Munich and Augsburg. Meteor. Z. 20 (1), 47–57.
Statheropoulos, M., Vassiliadis, N., Pappa, A., 1998. Principal component and canonical correlation analysis for examining air pollution and meteorological data. Atmos. Environ. 32 (6), 1087–1095.
Väkevä, M., Hämeri, K., Puhakka, T., Nilsson, E.D., Hohti, H., Mäkelä, J.M., 2000. Effects of meteorological processes on aerosol particle size distribution in an urban background area. J. Geophys. Res. 105 (D8), 9807–9821.
Viana, M., Querol, X., Alastuey, A., Gangoiti, G., Menéndez, M., 2003. PM levels in the Basque Country (Northern Spain): analysis of a 5-year data record and interpretation of seasonal variations. Atmos. Environ. 37 (21), 2879–2891.
Vogel, B., Groß, G., Wipper, F., 1986. MESOKLIP (first special observation period): observations and numerical simulation – a comparison. Bound.-Lay. Meteorol. 35 (1–2), 83–102.
Wang, M., Zhu, T., Zheng, J., Zhang, R.Y., Zhang, S., Xie, X., Han, Y., Li, Y., 2009. Use of a mobile laboratory to evaluate changes in on-road air pollutants during the Beijing 2008 Summer Olympics. Atmos. Chem. Phys. 9, 8247–8263.
Wehner, B., Wiedensohler, A., 2003. Long term measurements of submicrometer urban aerosols: statistical analysis for correlations with meteorological conditions and trace gases. Atmos. Chem. Phys. 3 (3), 867–879.
Weijers, E., Khlystov, A., Kos, G., Erisman, J., 2004. Variability of particulate matter concentrations along roads and motorways determined by a moving measurement unit. Atmos. Environ. 38 (19), 2993–3002.
Weimer, S., Mohr, C., Richter, R., Keller, J., Mohr, M., Prévôt, A., Baltensperger, U., 2009. Mobile measurements of aerosol number and volume size distributions in an Alpine valley: influence of traffic versus wood burning. Atmos. Environ. 43 (3), 624–630.
WHO, 2006. WHO Air Quality Guidelines for Particulate Matter, Ozone, Nitrogen Dioxide and Sulfur Dioxide – Global update 2005. WHO Press, Geneva, Switzerland.
Wieser, 2004. Messung turbulenter Spurengasflüsse vom Flugzeug aus. Dissertation. Universität Karlsruhe, Karlsruhe, Germany, p. 210.
Zahn, A., Weppner, J., Widmann, H., Schlote-Holubek, K., Burger, B., Kühner, T., Franke, H., 2012. A fast and precise chemiluminescence ozone detector for eddy flux and airborne application. Atmos. Meas. Tech. 5, 363–375.
van der Zee, S., Hoek, G., Harssema, H., 1998. Characterization of particulate air pollution in urban and non-urban areas in the Netherlands. Atmos. Environ. 32 (21), 3717–3729.